Temperature-Dependent Absorptances of Ceramics for Nd:YAG and CO_2 Laser Processing Applications

Z. Zhang and M. F. Modest
The Pennsylvania State University
University Park, PA 16802

Abstract

The absorptance of a material at the laser wavelength and as a function of temperature, ranging from room temperature to the removal point, significantly affects the efficiency of the laser machining process. *A priori* predictions of a laser machining process, using either simplistic or sophisticated models, requires knowledge of the material's absorptance behavior. An experimental apparatus for such measurements is described. The device consists of a specimen mounted inside an integrating sphere, heated rapidly by a CO_2 or a Nd:YAG laser. Reflectances are measured with a small focused probe laser (Nd:YAG or CO_2), while specimen surface temperatures are recorded by a high-speed pyrometer. Experimental results have been obtained for wavelengths of 1.06μm (Nd:YAG) and 10.6μm (CO_2) for graphite, alumina, hot-pressed silicon nitride, sintered α-silicon carbide, as well as two continous-fiber ceramic matrix composites (SiC-based). Data are presented for temperatures between room temperature and the ablation/decomposition points.

Introduction

Extensive application of lasers in materials processing has led to the development of several theoretical models to predict *a priori* the interaction between lasers and materials, e.g., [1–9]. These range from simple one-dimensional ones to complex three-dimensional transient models. To validate and use these models, the spectral absorptance of the material at the laser wavelength and at temperatures up to its ablation temperature is required. Currently, sufficient and accurate experimental data of this nature are not available. To measure the temperatures during laser processing, infrared pyrometry appears most suitable. However, since the temperature obtained by the pyrometer is the radiance temperature, knowledge of the emittance of the material at the pyrometer wavelength is again required to determine the actual temperature. In this article a new experimental set-up to rapidly determine high-temperature spectral absorptances at Nd:YAG and CO_2 wavelengths (1.06μm and 10.6μm), is presented. Results from these experiments can supply the necessary input data for the above theoretical models. Since pyrometers tend to operate around 1μm, the Nd:YAG absorptance measurements also provide the necessary emittance data for infrared pyrometry.

Various experimental techniques have been developed to measure the radiative properties of opaque materials. These may be separated into three loosely-defined groups: calorimetric emission measurements, radiometric emission measurements, and reflection measurements [10]. The calorimetric emission measurement methods and radiometric emission measurement methods

require the specimen to be maintained at the temperature, at which the radiative properties are to be measured. Therefore, it is unrealistic to measure the radiative properties of solids near their ablation temperature using these methods. Best suited for the present task with its extreme temperatures appears an integrating sphere reflectometer [11].

Jacquez and Kuppenheim [11] have provided the general theory of the integrating sphere for hemispherical spectral reflectance measurements. They describe two measurement techniques. In the first method, the so-called "substitution method," the reflected signal of the specimen and the standard reference are measured consecutively by replacing the sample by the standard, and the ratio of the respective detector readings is taken to determine the reflectance. In the second method, the so-called "comparison method," the sphere has two sample holders, and the sample and the standard reference are each placed in their own positions. The light beam is switched from sample to standard and the ratio of the respective detector readings is again determined. Efficiencies and errors for both methods were discussed by Jacquez and Kuppenheim.

Spectral hemispherical emittance measurements at high temperatures have been carried out by a number of researchers. One of the early works was done by Kneissl et al. [12]. Using an integrating sphere, they heated refractory metals and ceramics by induction up to 2000K. A He-Ne laser, which operated at several visible and near-infrared wavelengths was used together with corresponding bandpass filters to obtain high signal-to-noise ratios. A two-detector ratioing system was used to offset the power fluctuation of the He-Ne laser. Bober and co-workers [13–15] also measured the spectral emittance and reflectance of oxide and carbide ceramics up to 4000K at 0.663 and 10.6μm. They developed an integrating-sphere laser reflectometer, which used one laser beam for heating together with simultaneous irradiation of the specimen's surface by a second probe laser at a different wavelength. The probe laser was modulated by an ADP chopper and demodulated by a fast lock-in amplifier, which rejected the emission from the hot spot. The heating process took 100ms, which is the minimum to ensure temperature uniformity in the surface sublayer which absorbs and reflects thermal radiation from the probe laser. A simpler approach was used by Ramanathan and Modest [16], who used a single laser beam as both heating and probe light source. To smoothen out fluctuations in laser power, a thermopile detector was used for the reflectance measurements at the cost of temporal resolution.

In a reflectometer the energy falling onto the detector consists of two parts, the reflected radiation of the probe beam, the emitted radiation from the hot specimen, and, if a laser is used for heating, reflected radiation from the heating laser. The method adopted by Kneissl et al. [12] cannot reject the emission from the specimen and reflection from the heating laser completely. Bober et al. [13–15] used a combination of chopper and lock-in amplifier to overcome this problem, but they did not consider power fluctuations of the probe laser. In the scheme adopted by Ramanathan and Modest [16], their thermopile detector had a response time of 0.3s while the heating process took only 1s. This made it difficult for the detector to keep up with the changing signal, i.e., the detector may have lagged behind the changing signal, giving too flat a response. Another disadvantage of their scheme was that they used a single laser for both heating and probing. Therefore, the irradiated spot of the specimen was not isothermal due to the spatial laser beam profile as well as due to conduction losses. For a single beam the irradiation is reflected over a range of temperatures rather than at a single temperature, the highest temperature at the beam center being reported by the pyrometer. For this reason, the use of a single laser for both heating and probing can result in significant inaccuracy.

A new experimental apparatus for the rapid measurement of solid reflectance at high tem-

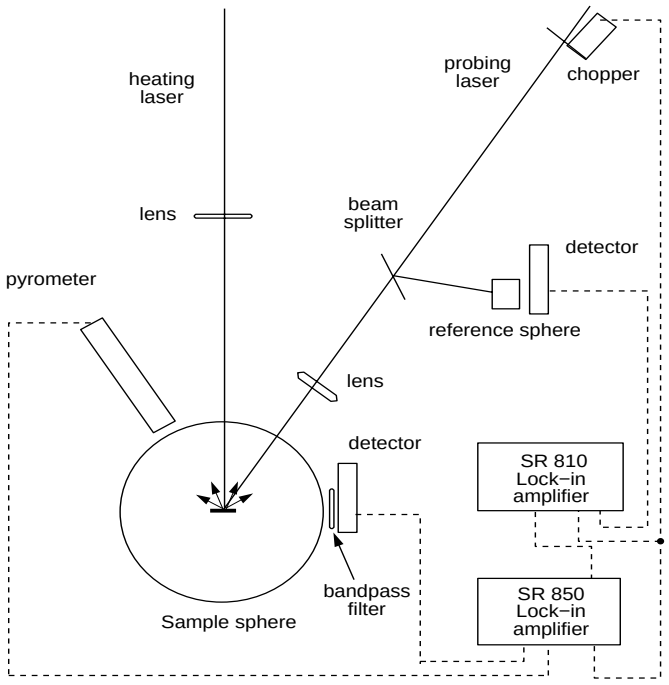

Figure 1: Shematic of experimental set-up.

peratures has been constructed. The set-up incorporates dual integrating spheres to eliminate power fluctuations of the probe light source, a combination of lock-in amplifier and chopper to reject emission from the specimen, and a separate heating laser at a different wavelength and with a substantially larger spot size to achieve an isothermal probed surface. A pyrometer with a spectral response of $0.8\sim1.0\mu$m was used to measure the sample temperature. The emittance of the material at the Nd:YAG wavelength was used to infer actual temperatures from the radiance temperature measured by the instrument. The absorptance as a function of temperature at Nd:YAG and CO_2 wavelengths is presented for several materials. The materials considered are graphite, α-silicon carbide, sintered silicon nitride, alumina, and two continuous-fiber composites, one with carbon fibers embedded in a silicon carbide matrix (C/SiC), and another with silicon carbide fibers embedded in a silicon carbide matrix (SiC/SiC).

Experimental Set-up

The experimental set-up for measuring the reflectance of a sample at elevated temperature is shown in Fig.1, consisting of two integrating spheres, a heating laser, a probe laser, two detectors, a mechanical chopper and two lock-in amplifiers and laser optics. The specimen was mounted at the center of the sample integrating sphere (RTC-060-IG), which was purchased from *Labsphere*. The inner wall of the sphere and the sample mount are coated with Infra-Gold, which has a reflectance of 95% over the range of $1\sim20\mu$m. The sample sphere is 15cm in diameter, has three 2.5cm access ports on the top, and another 1.25cm detector port is located at the side. The detector port is well baffled from the sample to ensure that the radiation is isotropically scattered before reaching the detector. The specimen was irradiated by a probe laser with an incidence angle of roughly 20^o, and

a beam diameter of approximately $100\sim200\mu$m. An *Apollo* 575 tunable CO_2 laser was used as probe laser for 10.6μm property measurements, while for 1.06μm a *Control* 512QG Nd:YAG laser was used. In each case, the probe laser beam was modulated by a mechanical chopper (SR540, *Stanford Research*) running at roughly 3kHz, near the maximum frequency of the chopper. The modulated signal was detected by an MCT detector (*Graseby Infrared*). This detector performs well at both 1.06 and 10.6μm. The detector was connected to the lock-in amplifier (SR850, *Stanford Research*). The modulation of the probe laser, together with a laserline bandpass filter in front of the detector to block the radiation at other wavelengths, allows the measurement of the reflected radiation in the presence of intense radiation emitted from the heated zone as well as reflection from the strong heating laser. The lock-in amplifier was set to run at a time constant of 1ms, which was restricted by the chopping frequency. In order to eliminate errors due to power fluctuation of the probe laser, the probe beam was split with a part of the beam going into a reference sphere. The signal of the reference sphere was picked up by another MCT detector (*Graseby Infrared*) and lock-in amplifier (SR810, *Stanford Research*).

The specimen was heated by a second laser operating at a different wavelength from the probe laser: during 1.06μm measurements, a CO_2 laser (*Coherent Everlase* S51) was used for heating, while a Nd:YAG laser (*Hobart* HLP 3000) was used for heating during 10.6μm property measurements. The sample sphere was purged with argon during the heating process to suppress chemical reactions. The heating laser was only partially focused to give a spot of roughly $1mm^2$. In this configuration the heating lasers were able to heat up the specimens to their ablation temperature within 100-200ms, which further minimized the chemical reactions. The probe laser was focused onto the center of the heated zone. First, the two lasers were aligned by using the internal alignment laser. Then both lasers were turned on to burn spots on a test sample. The alignment was adjusted to center the probe spot to the heating spot. Accurate alignment of the probe laser to the center of the considerably larger heated zone ensured that the probed spot was essentially isothermal.

To align the pyrometer for Nd:YAG probing, the probe laser spot location was determined using an IR viewer, afterwhich a He-Ne laser was focused onto the spot to indicate its position. For 10.6μm measurements the probe laser, when aimed at the specimen with the chopper off, was strong enough to heat the specimen to a temperature, whose emission was strong enough to be visible in the pyrometer's eyepiece, and the pyrometer was aligned to the center of this hot spot. The pyrometer was designed and constructed specifically for this experiment by Ramanathan et al. [17], and was aimed at the probe laser spot to measure the surface temperature of interest. The pyrometer has a viewing area of 50μm in diameter and time constant of 10μs. The spectral response of the pyrometer is approximately $0.8\sim1.1\mu$m. In order that the pyrometer can be used with a (heating or probe) Nd:YAG laser, a 0.95μm short-pass filter was added in front of the pyrometer. The pyrometer was recalibrated after the filter was added.

The demodulated reflection and temperature signals were digitally recorded. The specimen was then replaced by a standard reference with known reflectance without disturbing the set-up; only the probe laser was turned on this time and the radiation signals from both integrating spheres were recorded. The standard references used were a spectralon diffuse reflectance standard (SRS-99-010) and an Infra-Gold coated sample both purchased from *Labsphere*. The optics for the CO_2 laser path were made of zinc selenide, and the optics for the Nd:YAG laser path were made of calcium fluoride.

Jacquez and Kuppenheim [11] showed that for an integrating sphere with uniform wall coating the radiation, which passes out of an aperture of the sphere, is proportional to the specimen's

reflectance and a configuration coefficient, which is a function of the port area, the inner surface area of the sphere, and the reflectance of the wall coating. When the port area is small compared with the inner surface area of the sphere, which is an appropriate assumption for most integrating spheres, the configuration coefficient can be regarded as a constant. Furthermore, if the detectors are working at their linear range, it follows that

$$\frac{I_s}{I_r} = \frac{V_s}{V_r} = \frac{\rho_s}{\rho_r}, \tag{1}$$

where I_s and I_r are the intensities of the radiation, ρ_s and ρ_r are reflectances of the specimen and the reference, and V_s and V_r are signals produced by specimen and reference, respectively. For an opaque specimen, the spectral absorptance α and emittance ϵ is given by $\epsilon = \alpha = 1 - \rho_s$. Since temperature and reflectance signals are recorded simultaneously, they can be used together to provide absorptance versus temperature data. Because the pyrometer used has a radiance temperature range of 1500K to 3500K (after addition of the 0.95μm bandpass filter), the experiment cannot match the absorptance data to radiance temperatures below 1500K, although it still provides the value of absorptances at room temperature.

Results and Discussion

Between 4 and 6 different reflectance measurements were carried out at each wavelength for each material, using new specimens for each experiment. Each experiment was carried out at different power levels, to ascertain that there were no serious changes of reflectance with irradiation levels. It was observed, as done by Ramanathan and Modest [16] before, that the ablation temperature of each material increases somewhat with irradiation level; this is in qualitative agreement with an ablation rate according to an Arrhenius relation. Because of the limited number of runs, and because the maximum temperature reached in each experiment (but on the same material) was different, determination of standard deviations was deemed inappropriate. Instead, data for reflectance *vs.* radiance and actual temperatures are presented in terms of average values (averaging results from different irradiation powers), together with upper and lower bounds. For the highest temperatures, whenever less than three data points remained, only the average reflectance is shown.

Hot-pressed silicon nitride

The hot-pressed silicon nitride used in this study contains 6wt% Y_2O_3 and 2wt% Al_2O_3 as additives and was purchased from *GTE Inc*. Absorptance data for Si_3N_4 at 10.6μm and 1.06μm are shown in Figs.2 and 3 for temperatures up to its ablation temperature of approximately 2170K [18, 16]. The absorptance of Si_3N_4 at 1.06μm remains almost constant at 0.85 for temperatures all the way up to 2170K. The heating process shows the removal radiance temperature when the signal from the pyrometer reaches a constant as seen in Fig. 4 for a typical run . The radiance temperature during removal is seen to be approximately 2100K. Using the spectral emittance at 1.06μm, this yields an actual removal temperature of 2143K, which agrees well with the value provided by Pehlke and Elliot [18].

The absorptance at 10.6μm measured at room temperature with the present set-up was found to be 0.15, which is slightly lower than that reported by Roy et al. [19], who gave a value of 0.18. The absorptance remains low until about 1600K and beyond that changes appreciably with temperature. Si_3N_4 is known to have a reflection band at around 10μm [20]. The rapid increase of absorptance

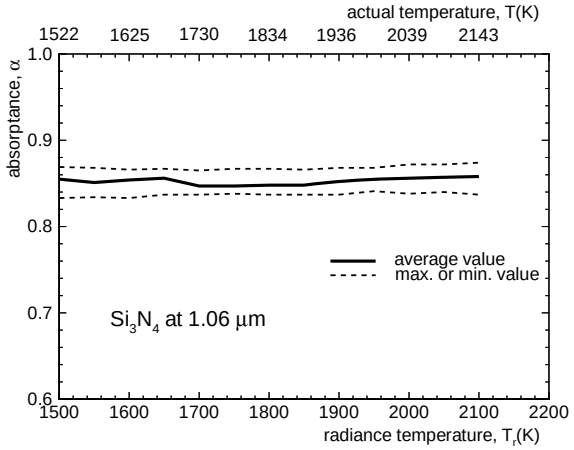

Figure 2: Absorptance *vs.* temperature of Si_3N_4 at 1.06μm.

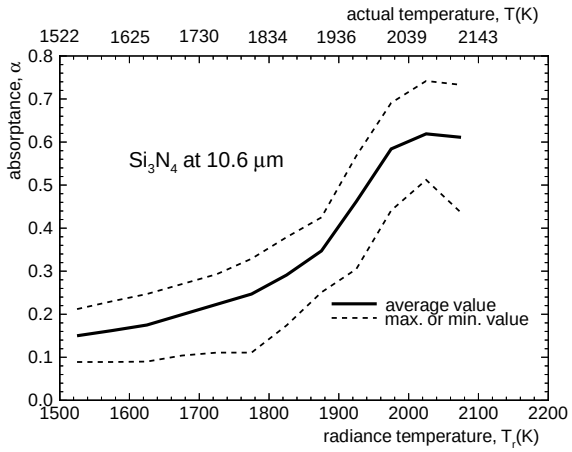

Figure 3: Absorptance *vs.* temperature of Si_3N_4 at 10.6μm.

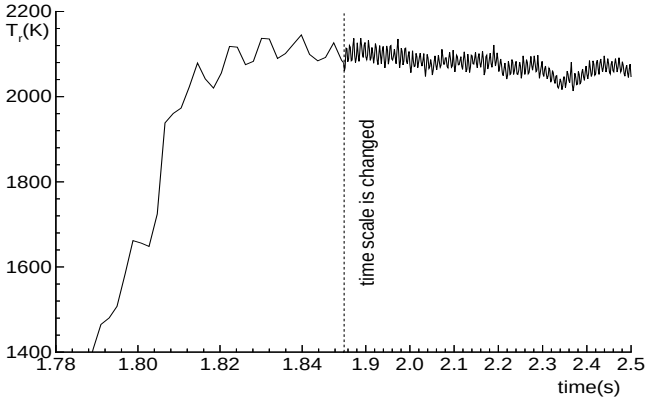

Figure 4: Typical temperature signal of Si_3N_4 during heating process.

can be attributed to a band shift at elevated temperatures. The present result is considerably different from that of Ramanathan and Modest [16], who reported that the absorptance increases only moderately as the temperature increases from 1300K to 2200K. As discussed earlier, due to the slow detector used in their experiment, their apparatus apparently did not respond fast enough to the rapidly changing signal.

Sintered α-silicon carbide

Sintered α-silicon carbide was purchased from *Carborundum Inc.*, in the form of a 3.5mm thick sheet. No data are available on the additives used in the manufacture of this material. The absorptance at 1.06μm increases slightly with temperature up to 2200K, after which it decreases to 0.73 at 2900K. SiC is known to have a 12.6μm reflection band [21] (fundamental lattice band), and the reflection band shifts to larger wavelengths as the temperature rises, as do other ionic crystals [22–24]. Because of the band shift one would expect to see a decrease in reflectance, and hence an increase in absorptance. Roy et al. [19] reported the normal absorptance of SiC at

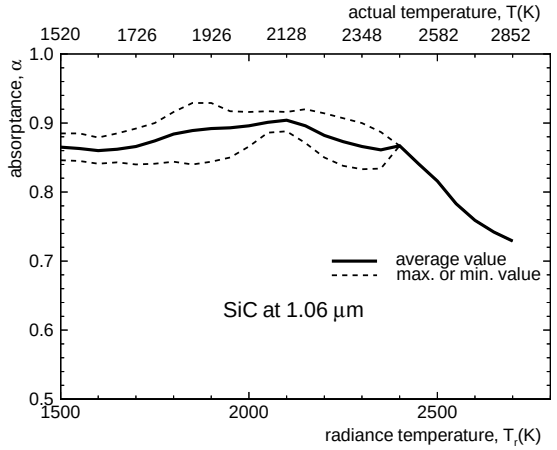

Figure 5: Absorptance *vs.* temperature of SiC at 1.06μm.

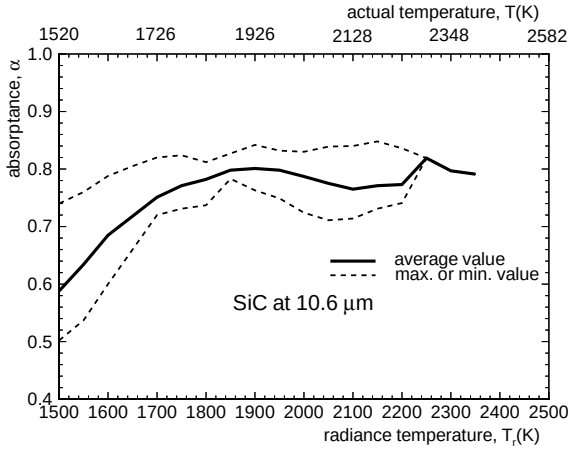

Figure 6: Absorptance *vs.* temperature of SiC at 10.6μm.

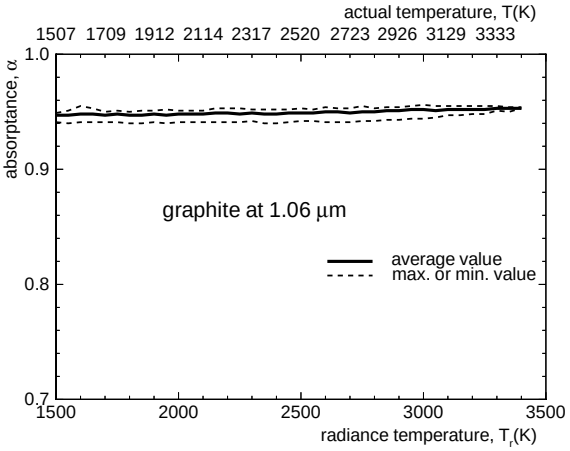

Figure 7: Absorptance *vs.* temperature of graphite at 1.06μm.

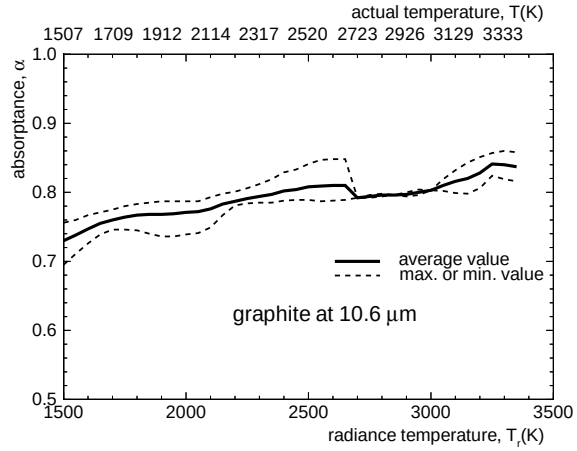

Figure 8: Absorptance *vs.* temperature of graphite at 10.6μm.

10.6μm to increase with temperature from 0.2 at room temperature to 0.85 at 1273K. Our data in Fig. 6 show that the absorptance at 10.6μm increases from 0.5 at 1500K to 0.83 at 1900K and then decreases marginally to 0.76. This difference may be attributed to the fact that Roy et al. [19] used equilibrium heating, which may have resulted in a thin SiO_2 layer on the surface, while laser heating takes only a fraction of a second, which minimizes chemical reactions.

Graphite

The graphite measured in this study is black graphite (*McMaster-Carr*). The absorptances at 1.06μm and 10.6μm are shown in Figs.7 and 8. The absorptance at 1.06μm is about 0.95 from 1500K to 3500K, which agrees well with the existing literature for the visible range [25]. On the other hand, the absorptance at 10.6μm shows a slight temperature dependence, increasing from 0.73 at 1500K to 0.84 at 3400K.

Alumina

The alumina used in this study was AD99 and was purchased from *Coors Corp*. Unlike all the

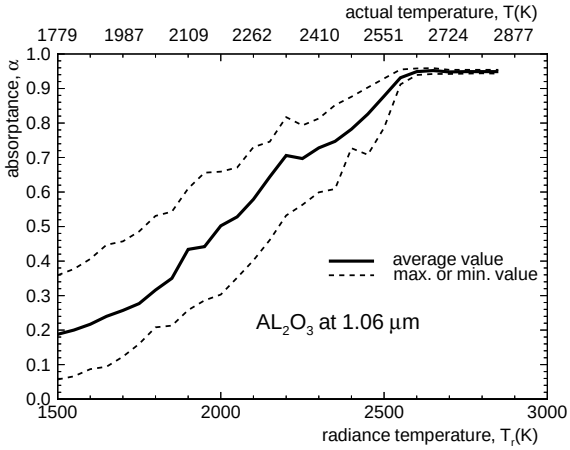

Figure 9: Absorptance *vs.* temperature of alumina at 1.06μm.

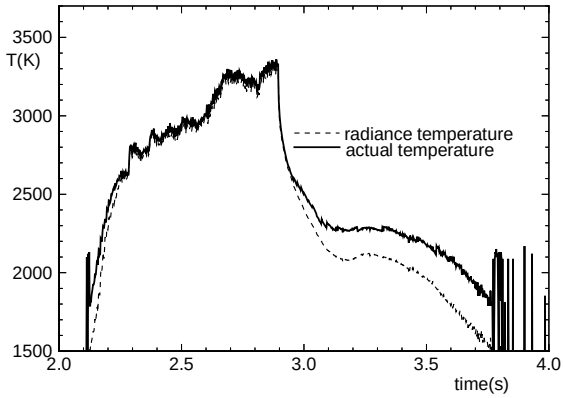

Figure 10: Typical temperature signal of alumina during heating process.

other ceramics in this study (which decompose mostly into gases without first melting), alumina is known to melt at around 2315K under equilibrium conditions [26]. The results presented in Fig. 9 are the absorptance at 1.06μm, showing that alumina is highly reflective until about 1800K, and its absorptance starts to increase sharply thereafter, reaching 0.95 at 2800K. The results differ from those of Blair [27], who used a "direct technique," which is known to be susceptible to large errors at short wavelengths [28]. Due to the low emittance at 1.06μm, the pyrometer could not detect temperatures below 1780K (or 1500K radiance temperature). Figure 9 does not show a distinct change in absorptance at the melting point of 2315K. Indeed, for most of the specimen the temperature *vs.* time signal did not show a distinct melting point. A typical temperature *vs.* time signal is shown in Fig. 10: because of the strong laser irradiation the alumina apparently superheats to about 2600K before starting to melt. Melting takes place over a range of temperatures and probably has not yet concluded when the laser was turned off at about 3350K. Note that during cool down there is a distinctive plateau at around 2300K, indicating equilibrium solidification and corroborating the JANAF table's melting temperature [26]. Data for the other specimens are similar, with onset of melting ranging from 2300K to 2600K, depending on irradiation levels. Results for 10.6μm are not available, since the absorptance of alumina at the heating laser wavelength of 1.06μm is only 0.18 in the temperature range between room temperature and 1800K. This causes large amounts of heat to be dissipated to the integrating sphere, which could damage the apparatus.

Composite materials

The composite materials considered were SiC/SiC composite (consisting of long woven β-silicon carbide fibers embedded in a β-silicon carbide matrix) and C/SiC composite (carbon fibers embedded in a β-silicon carbide matrix). They were obtained from *E.I. DuPont de Nemours and Co.*, and contained nominally 45 vol% matrix material and 45 vol% fibers, with the rest being porosity.

C/SiC Figures 11 and 12 show the absorptance of C/SiC at 1.06μm and 10.6 μm, respectively. The absorptance at 1.06μm increases slightly from 0.87 at 1550K to 0.92 at 3100K. This is slightly higher than that of monolithic α-silicon carbide and lower than that of graphite, which was expected. The absorptance at 10.6μm was found to be 0.7 at room temperature, which agrees with

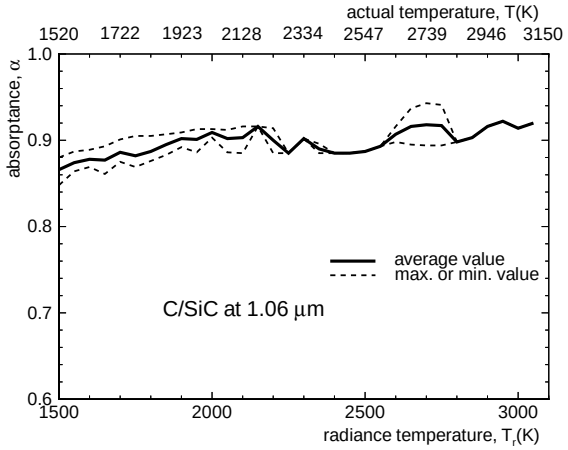

Figure 11: Absorptance *vs.* temperature of C/SiC at 1.06μm.

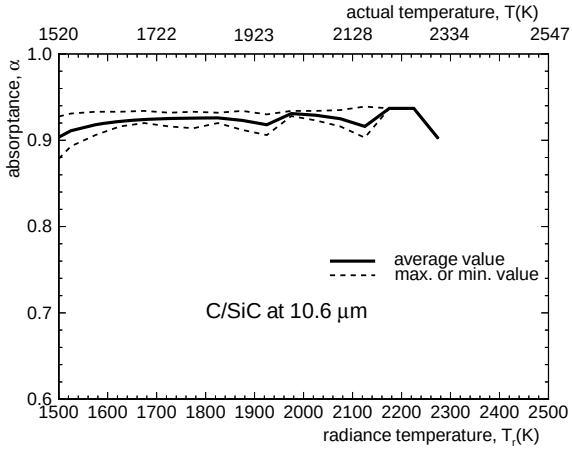

Figure 12: Absorptance *vs.* temperature of C/SiC at 10.6μm.

Ramanathan and Modest [16], who reported the absorptance at 10.6μm as 0.67 below 1250K, and increasing almost linearly with temperature to 0.77 at 2270K. The current study shows that the absorptance increases before the temperature reaches 1550K, and then changes slightly from 0.9 at 1550K to 0.93 at 2300K. Both inherent weaknesses of Ramanathan and Modest's scheme (single beam, slow detector) would tend to have their experiment report lower-than-actual absorptance data. The absorptance of C/SiC does not have the small peak around 2000K as the monolithic silicon carbide. This may be attributed to the fact that the decomposition of silicon carbide is suppressed by the carbon-rich vapors [29].

SiC/SiC Figures 13 and 14 show the spectral absorptance *vs.* temperature at 1.06μm and 10.6μm. At 1.06μm the absorptance shows no appreciable change with temperature. It is higher than that of monolithic SiC, which was expected due to the material's porosity. The absorptance at 10.6μm changes from 0.7 at 1700K to 0.92 at 2300K and then decreases to 0.72 at 2800K. As expected, these value are higher than those of Ramanathan and Modest [16], and also increase faster with temperature. The absorptance of SiC/SiC reaches a peak value at 2300K and decreases thereafter, which is consistent with the behavior of monolithic SiC. The peak at 2300K fades to a plateau of absorptance in Ramanathan and Modest [16]. It is also interesting to notice the peak of absorptance appearing around 2300K in contrast to that of C/SiC, which has no peak.

Conclusions

An integrating sphere reflectometer with dual laser beam heating and probing was constructed. The apparatus, which incorporates two integrating spheres in combination with a chopper and two lock-in amplifiers, can account for power fluctuations of the probe light source and measure the reflectance in the presence of intense ambient radiation. The hemispherical absorptances for a number of ceramics, namely silicon nitride, silicon carbide, graphite, alumina and two composite ceramics (C/SiC and SiC/SiC), have been presented. The results can furnish reliable radiative property data for use in theoretical models of laser processing, and can improve the accuracy of infrared pyrometry.

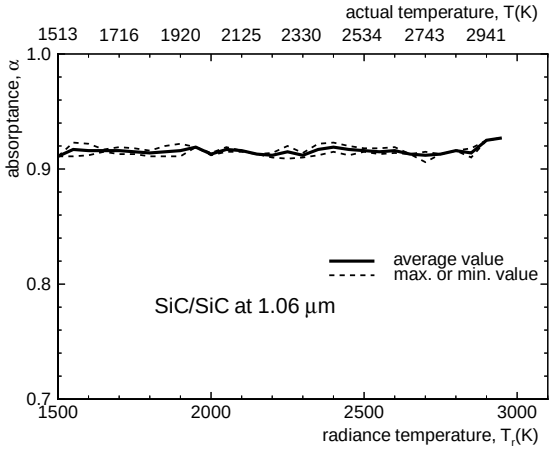

Figure 13: Absorptance *vs.* temperature of SiC/SiC at 1.06μm.

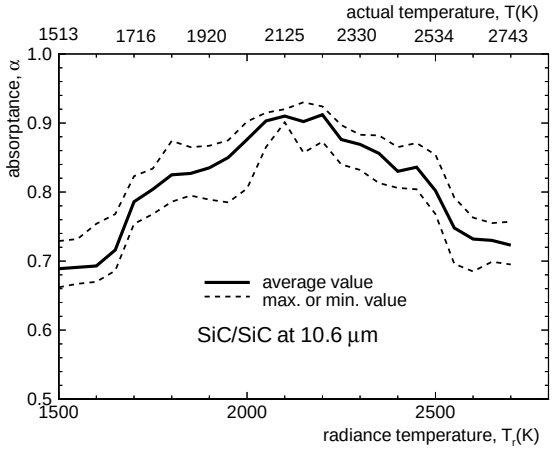

Figure 14: Absorptance *vs.* temperature of SiC/SiC at 10.6μm.

Acknowledgment

Support for this work by National Science Foundation Grant CTS-9312325 is gratefully acknowledged.

References

1. Dabby, F. W., and U.-C. Paek (1972), High-Intensity Laser-Induced Vaporization and Explosion of Solid Material, **IEEE J. Quantum Electron. QE-8**, 106–111.
2. Abakians, H., and M. F. Modest (1988), Evaporative Cutting of a Semi-Transparent Body with a Moving CW Laser, **J. Heat Transfer 110**, 924–930.
3. Chryssolouris, G. (1991), Laser Machining: Theory and Practice, Springer Verlag, New York, NY.
4. Vorreiter, J. O., D. A. Kaminski, and R. N. Smith (1991), MonteCarlo Simulation of a Laser Drilling Process, ASME paper no. 91-WA-HT-9.
5. Ramanathan, S., and M. F. Modest (1992), CW Laser Drilling of Composite Ceramics, In *Proceedings of ICALEO '91, Laser Materials Processing*, Vol. 74, 305–326, San Jose, CA.
6. Roy, S., and M. F. Modest (1993), CW Laser Machining of Hard Ceramics — Part I: Effects of Three-Dimensional Conduction and Variable Properties and Various Laser Parameters, **Int. J. Heat Mass Transfer 36**(14), 3515–3528.
7. Bang, S. Y., S. Roy, and M. F. Modest (1993), CW Laser Machining of Hard Ceramics — Part II: Effects of Multiple Reflections, **Int. J. Heat Mass Transfer 36**(14), 3529–3540.
8. Modest, M. F. (1996), Three-Dimensional, Transient Model for Laser Machining of Ablating/Decomposing Materials, **Int. J. Heat Mass Transfer 39**(2), 221–234.
9. Modest, M. F., S. Ramanathan, A. Raiber, and B. Angstenberger (December 1995), Laser Machining of Ablating Materials–Overlapped Grooves and Entrance/Exit Effects, **Journal of Laser Applications 7**(4), 210–218.
10. Modest, M. F. (1993), Radiative Heat Transfer, McGraw-Hill, New York.
11. Jacquez, J. A., and H. F. Kuppenheim (1955), Theory of the Integrating Sphere, **J. Opt. Soc. Am. 45**, 460–470.
12. Kneissl, G. J., and J. C. Richmond (1968), A Laser Source Integrating Sphere Reflectometer, Technical Report NBS-TN-439, National Bureau of Standards.
13. Bober, M. (1980), Spectral Reflectivity and Emissivity of Solid and Liquid UO_2 as a Function of Wavelength, Angle of Incidence, and Polarization, **High Temperatures - High Pressures 12**, 297–306.

14. Bober, M., and H. U. Karow (1977), Measurements of Spectral Emissivity of UO_2 above the Melting Point, In *Seventh Symposium on Thermophysical Properties* (Edited by Cezairlyian, A.), 344–350, National Bureau of Standards.
15. Bober, M., H. U. Karow, and K. Müller (1980), Study of the Spectral Reflectivity and Emissivity of Liquid Ceramics, **High Temperatures - High Pressures 12**, 161–168.
16. Ramanathan, S., and M. F. Modest (1993), Measurement of Temperatures and Absorptances for Laser Processing Applications, In *Proceedings of ICALEO '93, Laser Materials Processing*, 30–40, Orlando, FL.
17. Ramanathan, S., M. F. Modest, and Z. Zhang (1996), Design of a Fast Micro-Pyrometer for Laser Processing Applications, AIAA Paper no. 96-1885, Presented at AIAA 31st Thermophysics Conference, New Orleans, LA.
18. Pehlke, R. D., and J. F. Elliot (October 1959), High-Temperature Thermodynamics of the Silicon, Nitrogen, Silicon-Nitride System, **Transactions of the Metallurgical Society of AIME 215**, 781–785.
19. Roy, S., S. Y. Bang, M. F. Modest, and V. S. Stubican (1993), Measurement of Spectral, Directional Reflectivities of Solids at High Temperatures Between 9 and 11 μm, **Appl. Opt. 32**(19), 3550–3558.
20. Wallace, R. J. (1983), A Study of the Shaping of Hot Pressed Silicon Nitride With a High Power *CO_2 Laser*, PhD thesis, University of Southern California, Los Angeles, CA.
21. Spitzer, W. G., D. A. Kleinman, and D. J. Walsh (January 1959), Infrared Properties of Hexagonal Silicon Carbide, **Phys. Rev. 113**(1), 127–132.
22. Hass, M. (March 1960), Temperature Dependence of the Infrared Reflection Spectrum of Sodium Chloride, **Phys. Rev. 117**(6), 1497–1499.
23. Jasperse, J. R., A. Kahan, J. N. Plendl, and S. S. Mitra (1966), Temperature Dependence of Infrared Dispersion in Ionic Crystals LiF and MgO, **Phys. Rev. 140**(2), 526–542.
24. Chang, I. F., and S. S. Mitra (1972), Temperature Dependence of Long-Wavelength Optic Phonons of NaF Single Crystals, **Phys. Rev. B 5**(10), 4094–4101.
25. Wilson, R. J. (1964), Hemispherical Spectral Emittance of Ablation Chars, Carbon, and Zirconia, NASA-SP-55, Presented at Symp. on Thermal Radiation of Solids, San Francisco, CA.
26. Chase, J. M. W., C. A. Davies, J. J. R. Downey, D. J. Frurip, R. A. McDonald, and A. N. Syverud (Editors) (1985), JANAF Thermochemical Tables, National Bureau of Standards, Washington, DC.
27. Blair, R. (1960), Determination of Spectral Emissivity of Ceramic bodies at Elevated Temperature, **Journal of the American Ceramic Society 43**, 197–203.
28. Battuello, M., and T. Ricolfi (1989), A Technique for Deriving Emissivity Data for Infrared Pyrometry, **High Temperatures–High Pressures 21**, 303–309.
29. Singhal, S. C. (1976), Thermodynamic Analysis of the High-Temperature Stability of Silicon Nitride and Silicon Carbide, **Ceramurgia Int. 2**, 123–130.

Meet the Author

Zhaoyan Zhang is a doctoral graduate student in mechanical engineering at the Pennsylvania State University. Before coming to the U.S. he obtained his bachelor's and master's degrees in P. R. China in 1990 and 1995, respectively. Currently, he is doing research on radiative properties measurements relevant to laser material processing.

Michael F. Modest was born in Germany and received his Dipl.-Ing. degree in Mechanical Engineering from the Technical University in Munich in 1968. After emigrating to the U.S. he obtained his M.S. and Ph.D. degrees, also in Mechanical Engineering, from the University of California at Berkeley in 1972. He is presently a professor in the Mechanical Engineering Department at the Pennsylvania State University. His research interests cover two major areas in experiment as well as in theory: radiative heat transfer, and heat transfer during laser machining of ceramics.